ACS Photonics

Article

pubs.acs.org/journal/apchd5

Gigantic Optical Nonlinearity: Laser-Induced Change of Dielectric Permittivity of the Order of Unity

Guohua Zhu,[†] John. K. Kitur,[†] Lei Gu,[†] Jarrett Vella,[‡,§] Augustine Urbas,[∥] Evgenii E. Narimanov,[⊥] and Mikhail A. Noginov*,[†]

[†]Center for Materials Research, Norfolk State University, Norfolk, Virginia 23504, United States

[‡]Sensors Directorate and [∥]Materials and Manufacturing Directorate, Wright-Patterson Air Force Base, Dayton, Ohio 45433, United States

[§]Wyle, Dayton, Ohio 45431, United States

[⊥]Birck Nanotechnology Center, Department of Electrical and Computer Engineering, Purdue University, West Lafayette, Indiana 47907, United States

ABSTRACT: A possibility to tune optical properties of materials on demand is of great importance to both fundamental science and applications. We show that nanosecond laser pumping can significantly depopulate the ground state of AF455 dye nanoparticles, resulting in gigantic change of dielectric permittivity of the order of unity. Such extreme nonlinearity ($\chi^{(3)} = 1.3 \times 10^{-5}$ esu), evidenced by increase of the Mie scattering efficiency, places AF455 dye among the most efficient $\chi^{(3)}$ nonlinear optical materials, extends the limits of active metamaterials and plasmonics, and paves the way to ultimate control of photonic devices and systems.

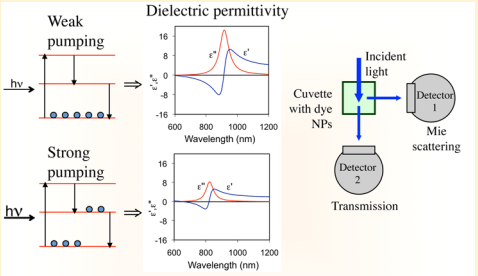

Laser-induced change of ground state concentration causes change of dielectric permittivity – strong Kerr effect. This, in turn, enhances Mie scattering and reduces transmission of the suspension of dye nanoparticles.

KEYWORDS: *nonlinear optics, optical materials, Kerr effect, dispersion, metamaterials*

Two classes of materials most commonly used in optics and photonics are low-loss dielectrics (including semiconductors) and metals. Their distinctly different optical properties, e.g. ability or inability to propagate light waves, are determined by their dielectric permittivities, $\tilde{\varepsilon} = \varepsilon' + i\varepsilon''$, whose real parts are positive in dielectrics, $\varepsilon' > 0$, and negative in metals, $\varepsilon' < 0$. Bringing metals and dielectrics in contact gives rise to localized and propagating surface plasmons, which stem from oscillation of free electrons at optical frequency and enable scores of fundamental physical phenomena and applications ranging from a spaser (plasmonic laser)[1] to surface-enhanced Raman scattering and sensing.[2]

Even broader range of unparalleled optical responses and fascinating applications, including negative index of refraction[3] and invisibility cloaking,[4] can be realized in photonic metamaterials,[5] artificial composite materials with rationally designed sizes, shapes, mutual orientations, and compositions of subwavelength inclusions, most commonly metals and dielectrics.

Most metamaterial and plasmonic systems (as well as optical materials in general) are passive. However, future devices and applications, for example, electronic circuits operating at optical frequencies,[6] call for active plasmonics and (meta)materials with optical gain,[7,8] nonlinearity,[9,10] and tunability.[11−19] Metamaterials can be tuned via changing dielectric permittivity $\tilde{\varepsilon}$ and magnetic permeability $\tilde{\mu}$ of constituent components or by physical reshaping. The majority of tuning mechanisms involve modifications of constituent materials which are (i) strong and slow or (ii) fast but small. The first category includes thermally or electrically induced reorientation of molecules in liquid crystals[11] and thermally induced phase transition in VO_2.[12] In these cases, the change of $\tilde{\varepsilon}$, $\tilde{\mu}$, or index of refraction $\tilde{n}$ can be large, >1, although, the switching rates typically do not exceed 100 Hz (here and below, $\tilde{n} = n + ik$). Tuning via mechanical reconfiguration of the metamaterial is usually slow, too.[13] However, 1 MHz switching rate has been reported in ref 14.

The second category of tuning mechanisms includes laser-induced nonlinearities,[15,16] saturable and reverse saturable absorption,[16] modification of dispersion determined by transient optical gain,[8,17,18] and fast laser-induced phase transitions (in chalcogenide glasses).[19] The characteristic times of such processes range from subpicosecond to 100 ns. However, the changes of $|\tilde{\varepsilon}|$, $|\tilde{\mu}|$, and $|\tilde{n}|$ are typically small, between ∼0.001 and ∼0.1. (Note that femtosecond laser-induced increase of electric conductivity of silica by 18 orders of magnitude, to reach that of semiconductors, has been reported in ref 20, and the ∼100 fs laser-induced phase transition in VO_2 has been reported in ref 21. To the best of our knowledge,

Received: January 12, 2015
Published: March 31, 2015

DOI: 10.1021/acsphotonics.5b00009
ACS Photonics 2015, 2, 622−627

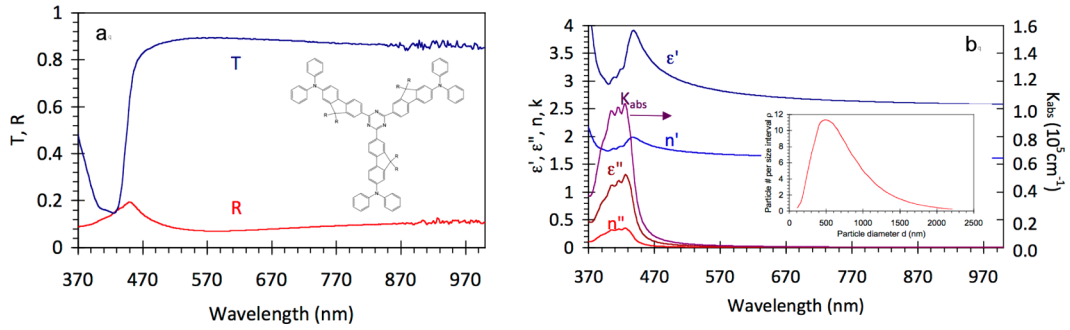

Figure 1. (a) Transmittance $T(\lambda)$ and reflectance $R(\lambda)$ spectra of the AF455 thin film. Inset: Chemical structure of the AF455 dye molecule. Adopted from ref 24. (b) Spectra of ε', ε'', n, k, and K_{abs} of the AF455 dye calculated from $T(\lambda)$ and $R(\lambda)$. The film thickness is 174 nm. Inset: size distribution of AF455 nanoparticles.

these processes have not been utilized in tunable metamaterials yet.)

Remarkably, strong control of plasmon and metamaterial responses, $|\Delta\tilde{\varepsilon}^{MM}| \sim |\Delta\tilde{\mu}^{MM}| \sim |\Delta\tilde{n}^{MM}| \sim 1$, can be achieved at much smaller changes of dielectric permittivity of interfacing constituent materials, $0.001 < |\Delta\tilde{\varepsilon}^{c}| \sim |\Delta\tilde{n}^{c}| < 0.1$.[8,15,18] The question arises whether a stronger (and fast) tuning of dielectric permittivity of constituent components can be realized experimentally in other systems, besides the two examples mentioned above,[20,21] and what kinds of nonlinear optical phenomena are expected in such an extreme regime, when ε' changes sign from positive (like in dielectric) to negative (like in metal). As we argue below, the later switchable metallic/dielectric plasmonic materials can not only revolutionize the whole research field of active metamaterials, but also have unique applications on their own.

To answer the first part of this question, we note that negative ε' can be found in the vicinity of strong absorption bands in concentrated laser dyes,[22] where a "perturbation" of real and imaginary parts of $\tilde{\varepsilon}$ can be as large as $\Delta\varepsilon'' \sim \Delta\varepsilon' \geq 5$. If the pumping pulse duration is longer than the excited state lifetime of the dye molecules τ, the fraction of ground state molecules n_g/N (in a three level or four level laser scheme) is given by

$$\frac{n_g}{N} \approx 1 - \frac{I\sigma\tau/\hbar\omega}{I\sigma\tau/\hbar\omega + 1} \quad (1)$$

where I is the pumping power density, σ is the absorption cross section, and $\hbar\omega$ is the photon energy. At dye emission cross section $\sigma = 4 \times 10^{-16}$ cm^2 and emission lifetime $\tau = 4$ ns, modest laser dye parameters, more than 50% of dye molecules can be excited with 5 ns laser pulses ($\lambda = 500$ nm) at the pumping density $\geq$1.2 mJ/cm^2. This value is easy to achieve and, if needed, it can be exceeded by an order of magnitude or more, implying that the molecule ground state can be efficiently depopulated even at shorter emission life times expected of highly concentrated dyes. Therefore, laser-induced change of ε' in organic media by more than one, $\Delta\varepsilon' > 1$, does not seem to be an impossible task.

Given that such a strong control of dielectric permittivity is, indeed, possible, one can predict unparalleled material properties and applications, which have been absolutely unthinkable so far. Thus, by tuning dielectric permittivity of a material from a dielectric state, $\varepsilon' > 0$, to a metallic state, $\varepsilon' < 0$, one can gain unprecedented control over photonic and plasmonic waves,[23] for example, to switch a waveguide from a photonic mode to a plasmonic mode.

Furthermore, negative dielectric permittivity of an organic dye can be achieved not only in the vicinity of a very strong absorption band, but also in the vicinity of an equally strong gain band. Such material, which simultaneously has negative real and imaginary parts of dielectric permittivity can be regarded as a "metal with gain", a unique active medium that has never been realized or discussed in the literature. One of its potential uses is in a new-generation spaser, which will not have a traditional metallic core supporting plasmon oscillation[1] (an inevitable source of a strong absorption loss), but will consist of a single phase nanoparticle with $\varepsilon' < 0$ and $\varepsilon'' < 0$, providing for both gain and stimulated emission feedback. With no doubts, optical material with such strong (and fast) tunability can revolutionize the whole area of metamaterials (if used as a constituent component), plasmonics and nanophotonics. In this Letter, we report on the first step taken in this direction, nanosecond laser control of dielectric permittivity of dye nanoparticles of the order of $|\Delta\varepsilon| \approx 1$.

Experimentally, we have studied nanoparticles and thin films of the AF455 dye,[24] inset of Figure 1a. In many highly concentrated dyes, the population inversion and corresponding substantial changes in the spectra of dielectric permittivity are difficult to achieve because of strong concentration quenching. To avoid the quenching problem, the nanoparticles and films consisting of the triazine based AF455 compound have dye molecules cores separated by alkyl side chains, resulting in the luminescence quantum yield as high as 0.1. The synthesis, structure, and spectroscopic properties of this material are described in ref 25. Dye nanoparticles were prepared, similar to ref 26, by dispersing a 3% (by weight) acetone solution of AF455 into water at 40 °C under sonication. The alkyl spacer side chains prevent the AF455 compound from aggregating or crystallizing. Thus, spherical amorphous particles have been obtained. Thin films were spin coated onto glass substrates for 60 s at 3000 rpm from a 3% (by weight) solution of AF455 in toluene. The samples were allowed to dry for 24 h before spectral measurements.

The transmittance, $T(\lambda)$, and reflectance, $R(\lambda)$, spectra of the AF455 thin films deposited on glass have been measured in the Lambda 900 spectrophotometer setup, Figure 1a. The known formulas[27] (modified Frensel equations) relate the reflectance and transmittance spectra to the spectra of real and imaginary parts of $\tilde{\varepsilon}(\lambda)$. Correspondingly, if the spectrum $\tilde{\varepsilon}(\lambda)$ is modeled as a combination of several Lorentz oscillators,

$$\tilde{\varepsilon}(\omega) = \varepsilon_h + \sum_j \frac{A_j}{\omega_j^2 - \omega^2 - i\omega/\tau_j} \quad (2)$$

DOI: 10.1021/acsphotonics.5b00009
ACS Photonics 2015, 2, 622–627

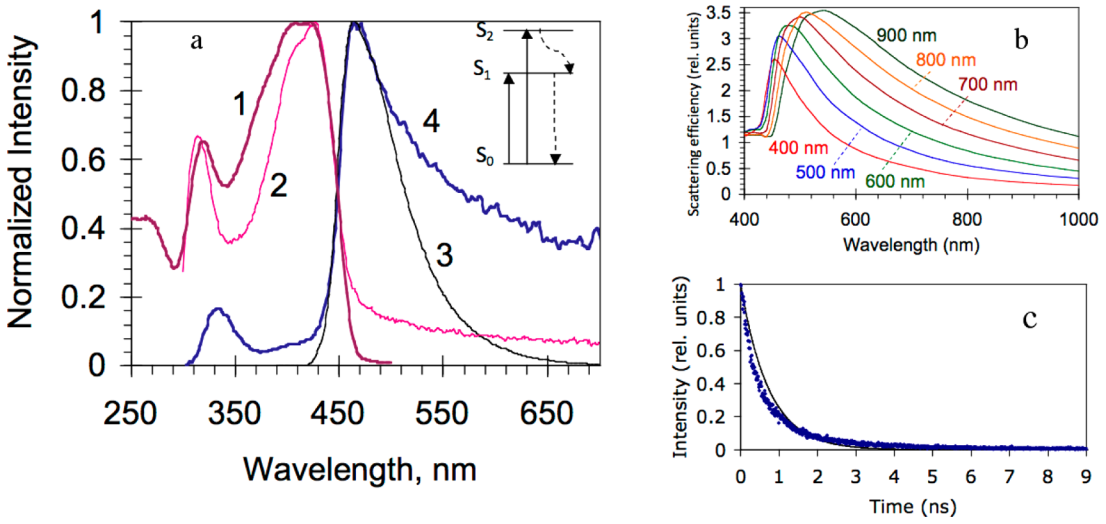

Figure 2. (a) Absorbance (1), excitation (2), emission (3), and Mie scattering spectra (4) of the water suspension of AF455 nanoparticles. Inset: energy state diagram of AF455. (b) Mie scattering spectra calculated for different particle sizes. (c) Emission kinetics: dots, experiment; solid line, exponential fit with τ = 0.73 ns.

the parameters ε_h, ω_j, τ_j, and A_j, as well as the film thickness d, can be varied to get the best fit between the experimental and the calculated spectra $R(\lambda)$ and $T(\lambda)$. Here ω is the angular frequency, ε_h is the real dielectric permittivity of the host medium, ω_j and τ_j are the central frequency and the relaxation time of the j^{th} oscillator, and A_j is the amplitude factor.

The spectra of ε' and ε'' (modeled as a combination of six Lorentzian line-shapes) obtained in result of such fitting procedure are shown in Figure 1b. As one can see, in the vicinity of the absorption line at $\lambda \sim 0.42$ μm - 0.45 μm, ε' and ε'' vary approximately by 1, suggesting that equally strong changes of dielectric permittivity can be expected at sufficiently strong laser pumping, which significantly depopulates the ground state of the dye molecules. The spectra of real, n, and imaginary, k, parts of the refractive index are depicted Figure 1b, along with the spectrum of absorption coefficient, K_{abs}. Knowing the density of the AF455 dye, ρ = 0.95 g/cm^3, and its molecular weight, MW = 1917 g/mol,[28] one can calculate the concentration of AF455 molecules, $N = 3.0 \times 10^{20}$ cm^{-3}, in solid dye compound and the peak absorption cross section, $\sigma^{\max} = 3.5 \times 10^{-16}$ cm^2 at λ = 426 nm.

Note that larger number of Lorentzian profiles used in the fitting procedure would result in smoother spectra. The fact that Lorentz oscillators were used to model the spectrum of dielectric permittivity $\tilde{\varepsilon}(\lambda)$ guarantees that $\varepsilon'(\lambda)$ and $\varepsilon''(\lambda)$ match each other via the Kramers−Kronig relations and do not violate causality.

Water suspension of dye nanoparticles had lightly greenish and scattering appearance. The broad size distribution of the nanoparticles $\rho(d)$ was measured using elastic light scattering technique. The maximum of the distribution was at $d_{\max} \approx 500$ nm and the average (expectation) value of the diameter d_0, defined as $\int_0^{d_0}\rho(x)\mathrm{d}x = \int_{d_0}^{0}\rho(x)\mathrm{d}x$, was equal to ≈660 nm, inset of Figure 1b.

Emission, excitation, and Mie scattering spectra of the water suspension of AF455 nanoparticles were recorded in the spectrofluorimeter setup (Fluoromax 3). In the emission measurements, the excitation wavelength was kept constant, λ_{ex} = 395 nm, and the emission wavelength was scanned; while in the excitation measurements, the excitation wavelength was scanned and the emission wavelength was kept constant, λ_{em} = 520 nm. In the Mie scattering measurements, excitation and collection monochromators were scanned synchronously. Both emission and scattering signals were detected in the direction orthogonal to the excitation light beam. These spectra, along with the absorption spectrum measured in the spectrophotometer, are shown in Figure 2a.

The absorption and excitation spectra, nearly identical to each other, are dominated by the band centered at 0.42 μm, corresponding to the transition between the singlet ground state S_0 and first excited state S_1,[24] see Figure 2a and inset. The second band with the maximum at 0.32 μm is tentatively assigned to the transition $S_0 \rightarrow S_2$.[24] The strong emission band with the maximum at 0.47 μm (at the transition $S_1 \rightarrow S_0$) is Stokes shifted relative to the corresponding absorption band, Figure 2a. The emission originating at the second excited state S_2 is almost completely quenched, probably due to strong nonradiative relaxation $S_2 \rightarrow S_1$. The Mie scattering spectrum has two maxima red-shifted in respect to the corresponding absorption bands, Figure 2a. The Mie spectra calculated for several particle sizes (Figure 2b) based on the spectra of dielectric permittivity (Figure 1b) resemble the experimental spectrum (Figure 2a).[29]

Absolute measurements of the emission quantum yield in AF455 dye nanoparticles (based on comparison of the emission intensity and the excitation intensity) were carried out using an integrating sphere with the Horiba Jobin-Yvon Fluorolog-3 spectrometer, as described in ref 30. At the excitation wavelength λ = 429 nm, the quantum yield was evaluated to be equal to η = 0.1.

In the emission kinetics measurements, AF455 nanoparticles were excited by 70 ps laser pulses at λ = 375 nm. The emission signal was spectrally filtered and detected using the Edinburgh OB920 fluorescence spectrometer equipped with the time correlated single photon counting detector. The effective decay time τ, defined as $\int_0^\infty \exp(-t/\tau)\mathrm{d}t = \int_0^\infty I(t)\mathrm{d}t$ was equal to 0.73 ns, Figure 2c.

In the last and the most important experiment of this study, the suspension of dye nanoparticles, placed in a cuvette with square (1 cm x 1 cm) cross section and four polished walls, was excited with 4 ns pulses of the optical parametric oscillator at λ

DOI: 10.1021/acsphotonics.5b00009
ACS Photonics 2015, 2, 622−627

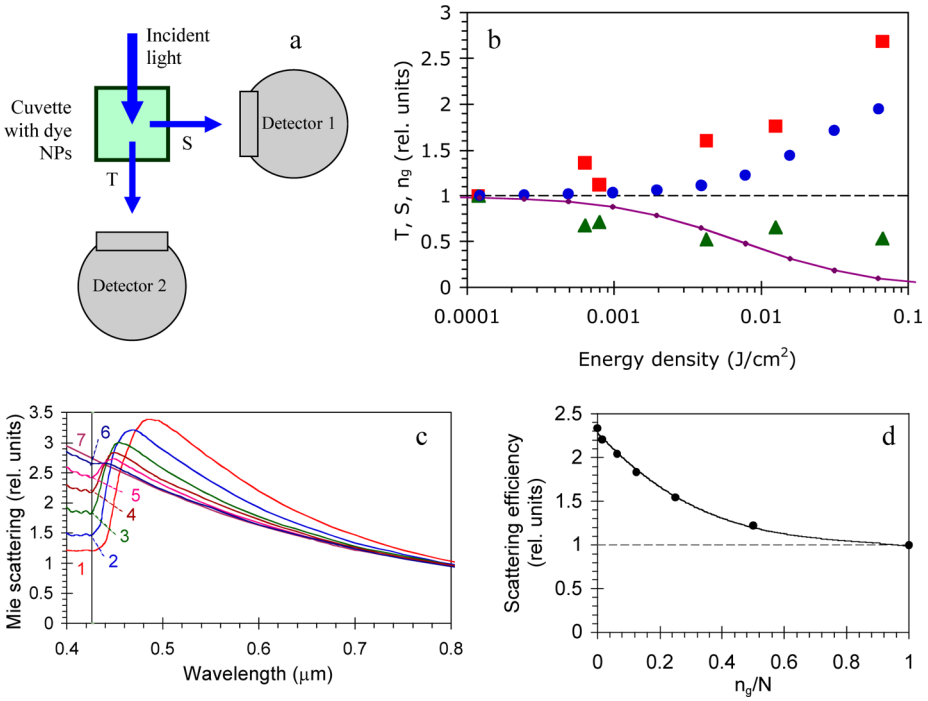

Figure 3. (a) Schematic of transmission and scattering measurements. (b) Experimental Mie scattering efficiency (red squares), experimental transmission (green triangles), calculated Mie scattering (blue circles), and calculated ground state population n_g/N (solid line). Inset: The dependence of ε' and n on the pumping energy density calculated at λ = 436 nm, based on eqs 1 and 2 and the spectra of Figure 1b. (c) Mie scattering spectra calculated for d = 0.66 μm and n_g/N equal to 1 (1), 1/2 (2), 1/4 (3), 1/8 (4), 1/16 (5), 1/64 (6), and 0 (7). (d) Calculated scattering efficiency (at λ = 426 nm) as a function of n_g/N.

= 426 nm. Experimentally, the sample's transmission (T) and Mie scattering (S) were measured, in the setup of Figure 3a, as the function of the pumping density, which was varied using a set of neutral density filters over nearly 3 orders of magnitude. We found that with increase of the pumping density from 0.12 to 67 mJ/cm^2, the Mie scattering efficiency increased nearly 3-fold, Figure 3b. (The latter was defined as the Mie scattering intensity measured with Detector 1, Figure 1a, divided by the pumping density.) At the same time, the sample's transmittance, measured with Detector 2 (Figure 3a), decreased approximately 2-fold, Figure 3b. The observation of the strong laser-induced change of the scattering efficiency and transmittance is the central result of this study.

As we show below, both effects stem from strong laser-induced depopulation of the ground state of the AF455 molecules and corresponding gigantic change of dielectric permittivity, $\Delta|\tilde{\varepsilon}| \sim 1$. In fact, at the experimentally determined absorption cross section of the dye molecules in solid state, σ = 3.5 × 10^{-16} cm^2, spontaneous emission lifetime τ = 0.73 ns, pumping pulse duration t_p = 4 ns[31] and excitation wavelength λ = 426 nm, the saturation energy density (at which $I\sigma/\hbar\omega = 1/\tau$) can be evaluated as $E_s = I_s t_p$ = 7.3 mJ/cm^2. Correspondingly, at the maximal pumping energy density available in our experiment, 67 mJ/cm^2, the ground state population was nearly depleted, n_g/N = 0.10.

As the ground state concentration is getting smaller, the numerators of Lorentzian terms in eq 2 decrease accordingly ($A_j \propto n_g/N$), leading to smaller minimum-to-maximum variation in the spectra of $\varepsilon'(\lambda)$ and $\varepsilon''(\lambda)$. (We neglect any contribution to dispersion originating from population of excited states.) This causes change in the Mie scattering spectra, in particular, strong enhancement of the scattering efficiency at the pumping wavelength, λ = 426 nm, Figure 3c. The calculations predict that, as n_g/N decreases from 1 to 0 and $\Delta|\tilde{\varepsilon}|$ changes by ~1 (Figure 1b), the scattering efficiency (calculated at 426 nm for average particle size d_0 = 0.66 μm) increases 2.0×, which is reasonably close to the 2.7-fold enhancement measured experimentally. The calculated dependence of the scattering efficiency S on the ground state population n_g/N is plotted in Figure 3d. Combining the dependence of n_g/N on the pumping energy density $E = It_p$, which can be calculated from eq 1, with the dependence of the scattering efficiency S on n_g/N, depicted in Figure 3d, one can calculate the dependence of S on E (Figure 3b, blue circles). One can see that the latter is in fair agreement with the experimental result (Figure 3b, red squares). The relatively small discrepancy between the theory and the experiment can be explained by, for example, approximation of emission kinetics with a single exponent, overestimation of the pulse duration t_p, and imperfect spherical shapes of dye nanoparticles, which were assumed to be spherical in the Mie calculation. The increase of the Mie scattering explains the reduction of transmission at increase of the pumping energy (Figure 3b, green triangles): the larger number of photons is scattered, the smaller number of photons is transmitted.

Lastly, inferring that the amplitude of the "wavelike" perturbation in the spectrum of the refraction index n at λ = 0.42−0.45 μm (Figure 1b) is proportional to the ground state population n_g/N, which, in turn, depends on the pumping power density I, one can present n in the standard Kerr nonlinearity form $n = n_0 + n_2 I$, where n_2 = 1.9 × 10^{-7} cm^2/W. (The estimate is made at small pumping intensities I, at which change of n is linearly proportional to I, see inset of Figure 3b.) The corresponding third order susceptibility $\chi^{(3)}$ = 1.3 × 10^{-5} esu, combined with the nanosecond time response $t \sim$ 0.7 ns, places AF455 dye among the most advanced $\chi^{(3)}$ nonlinear

DOI: 10.1021/acsphotonics.5b00009
ACS Photonics 2015, 2, 622−627

optical materials, including Au ($\chi^{(3)} = 10^{-8}$ esu, $t \sim 90$ fs),[32] graphene ($\chi^{(3)} = 4 \times 10^{-7}$ esu, $t \sim 6$ ps),[33] polydiacetilene (at peak of excitation, $\chi^{(3)} = 7.5 \times 10^{-6}$ esu, $t \sim 2$ ps),[34] GaAs ($\chi^{(3)} = 6.5 \times 10^{-4}$ esu, $t \sim 20$ ns),[34] GaAs/GaAlAs quantum wells ($\chi^{(3)} = 4 \times 10^{-2}$ esu, $t \sim 20$ ns),[34] and InSb (77 K, 5.4 μm, $\chi^{(3)} = 3 \times 10^{-1}$ esu, $t \sim 400$ ns).[34] (Note that following ref 34, the (effective) third order succeptibilities $\chi^{(3)}$ above are formally related to n_2, with the formula, n_2 (cm^2/W) = $(12\pi^2/n_0^2c)10^7\chi^{(3)}$(esu), and not all of them, especially those characterizing slow processes, can enable two-photon absorption or harmonics generation.)

To summarize, we have studied spectroscopic and nonlinear properties of thin films and nanoparticles of the AF455 dye. We estimate that, at modest pumping energy density used in our experiment, 67 mJ/cm^2, the ground state of molecules was almost completely depopulated, $n_g/N = 0.10$, leading to the change of dielectric permittivity of the order of $\Delta|\tilde{\varepsilon}| \sim 1$. This results in nearly 3-fold increase of the Mie scattering efficiency as the pumping energy density is raised from 0.12 to 67 mJ/cm^2. The corresponding gigantic optical nonlinearity, $\chi^{(3)} = 1.3 \times 10^{-5}$ esu, of a solid state organic compound at nanosecond laser pumping is of imminent importance to nonlinear optics, metamaterials, and plasmonics. This is also the first step toward novel photonic materials with unparalleled responses to electromagnetic waves, which can be tuned to metallic, dielectric, or epsilon near zero states on demand or even combine properties of metals and gain media, leading to metalless spasers and other applications, which are unthinkable with currently available materials.

AUTHOR INFORMATION

Corresponding Author

*E-mail: mnoginov@nsu.edu.

Notes

The authors declare no competing financial interest.

ACKNOWLEDGMENTS

The authors acknowledge NSF PREM Grant DMR 1205457, AFOSR Grant FA9550−14−1−0221, NSF IGERT Grant DGE 0966188, ARO Grant W911NF-14−1−0639, ARO MURI, NSF Center for Photonics and Multiscale Nanomaterials, and Gordon and Betty Moore Foundation.

REFERENCES

(1) Bergman, D.; Stockman, M. Surface Plasmon Amplification by Stimulated Emission of Radiation: Quantum Generation of Coherent Surface Plasmons in Nanosystems. *Phys. Rev. Lett.* **2003**, 90.

(2) Kneipp, K.; Wang, Y.; Kneipp, H.; Perelman, L.; Itzkan, I.; Dasari, R.; Feld, M. Single Molecule Detection Using Surface-Enhanced Raman Scattering (SERS). *Phys. Rev. Lett.* **1997**, *78*, 1667−1670.

(3) Veselago, V. The electrodymamics of substances with simultaneously negative values of ε and μ. *Sov. Phys. Usp.* **1968**, *10*, 509−514.

(4) Pendry, J. Controlling Electromagnetic Fields. *Science* **2006**, *312*, 1780−1782.

(5) Noginov, M.; Podolskiy, V. *Tutorials In Metamaterials*; Taylor & Francis: Boca Raton, FL, 2012.

(6) Engheta, N. Circuits With Light At Nanoscales: Optical Nanocircuits Inspired By Metamaterials. *Science* **2007**, *317*, 1698−1702.

(7) Sudarkin, A.; Demkovich, P. Excitation of Surface Electromagnetic Waves on the Boundary of a Metal with an Amplifying Medium. *Tech. Phys.* **1989**, *34*, 764−766.

(8) Noginov, M.; Podolskiy, V.; Zhu, G.; Mayy, M.; Bahoura, M.; Adegoke, J.; Ritzo, B.; Reynolds, K. Compensation of Loss in Propagating Surface Plasmon Polariton by Gain in Adjacent Dielectric Medium. *Opt. Express* **2008**, *16*, 1385.

(9) Kauranen, M.; Zayats, A. Nonlinear Plasmonics. *Nat. Photonics* **2012**, *6*, 737−748.

(10) Liu, Y.; Bartal, G.; Genov, D.; Zhang, X. Subwavelength Discrete Solitons in Nonlinear Metamaterials. *Phys. Rev. Lett.* **2007**, *99*.

(11) Xiao, S.; Chettiar, U.; Kildishev, A.; Drachev, V.; Khoo, I.; Shalaev, V. Tunable Magnetic Response of Metamaterials. *Appl. Phys. Lett.* **2009**, *95*, 033115.

(12) Dicken, M.; Aydin, K.; Pryce, I.; Sweatlock, L.; Boyd, E.; Walavalkar, S.; Ma, J.; Atwater, H. Frequency Tunable Near-Infrared Metamaterials Based on VO_2 Phase Transition. *Opt. Express* **2009**, *17*, 18330.

(13) Pryce, I.; Aydin, K.; Kelaita, Y.; Briggs, R.; Atwater, H. Highly Strained Compliant Optical Metamaterials With Large Frequency Tunability. *Nano Lett.* **2010**, *10*, 4222−4227.

(14) Ou, J.; Plum, E.; Zhang, J.; Zheludev, N. An Electromechanically Reconfigurable Plasmonic Metamaterial Operating in the near-Infrared. *Nat. Nanotechnol.* **2013**, *8*, 252−255.

(15) Cho, D.; Wu, W.; Ponizovskaya, E.; Chaturvedi, P.; Bratkovsky, A.; Wang, S.; Zhang, X.; Wang, F.; Shen, Y. Ultrafast Modulation Of Optical Metamaterials. *Opt. Express* **2009**, *17*, 17652.

(16) Christodoulides, D.; Khoo, I.; Salamo, G.; Stegeman, G.; Van Stryland, E. Nonlinear Refraction And Absorption: Mechanisms And Magnitudes. *Adv. Opt. Photonics* **2010**, *2*, 60.

(17) Govyadinov, A.; Podolskiy, V.; Noginov, M. Active Metamaterials: Sign Of Refractive Index And Gain-Assisted Dispersion Management. *Appl. Phys. Lett.* **2007**, *91*, 191103.

(18) Xiao, S.; Drachev, V.; Kildishev, A.; Ni, X.; Chettiar, U.; Yuan, H.; Shalaev, V. Loss-Free And Active Optical Negative-Index Metamaterials. *Nature* **2010**, *466*, 735−738.

(19) Samson, Z.; MacDonald, K.; De Angelis, F.; Gholipour, B.; Knight, K.; Huang, C.; Di Fabrizio, E.; Hewak, D.; Zheludev, N. Metamaterial Electro-Optic Switch Of Nanoscale Thickness. *Appl. Phys. Lett.* **2010**, *96*, 143105.

(20) Schiffrin, A.; Paasch-Colberg, T.; Karpowicz, N.; Apalkov, V.; Gerster, D.; Mühlbrandt, S.; Korbman, M.; Reichert, J.; Schultze, M.; Holzner, S.; et al. Optical-Field-Induced Current In Dielectrics. *Nature* **2012**, *493*, 70−74.

(21) Cavalleri, A.; Toth, C.; Siders, C.; Squier, J.; Ráksi, F.; Forget, P.; Kieffer, J. Femtosecond Structural Dynamics In VO_2 During An Ultrafast Solid-Solid Phase Transition. *Phys. Rev. Lett.* **2001**, *87*.

(22) Gu, L.; Livenere, J.; Zhu, G.; Narimanov, E.; Noginov, M. Quest For Organic Plasmonics. *Appl. Phys. Lett.* **2013**, *103*, 021104.

(23) Atwater, H. The Promise of Plasmonics. *Sci. Am.* **2007**, *17*, 56−63.

(24) Rogers, J.; Slagle, J.; McLean, D.; Sutherland, R.; Sankaran, B.; Kannan, R.; Tan, L.; Fleitz, P. Understanding The One-Photon Photophysical Properties Of A Two-Photon Absorbing Chromophore. *J. Phys. Chem. A* **2004**, *108*, 5514−5520.

(25) Kannan, R.; He, G.; Lin, T.; Prasad, P.; Vaia, R.; Tan, L. Toward Highly Active Two-Photon Absorbing Liquids. Synthesis And Characterization Of 1,3,5-Triazine-Based Octupolar Molecules. *Chem. Mater.* **2004**, *16*, 185−194.

(26) Kasai, H.; Nalwa, H.; Oikawa, H.; Okada, S.; Matsuda, H.; Minami, N.; Kakuta, A.; Ono, K.; Mukoh, A.; Nakanishi, H. A Novel Preparation Method Of Organic Microcrystals. *Jpn. J. Appl. Phys.* **1992**, *31*, L1132−L1134.

(27) Raether, H. *Surface Plasmons on Smooth and Rough Surfaces and on Gratings*; Springer-Verlag: Berlin, 1988.

(28) Sutherland, R.; Brant, M.; McLean, D.; Rogers, J.; Sankaran, B.; Kirkpatrick, S.; Fleitz, P. Photophysics of Organic Materials Exhibiting Strong Two-Photon and Excited State Absorption; Nonlinear Optical Transmission and Multiphoton Processes in Organics II. *Proc. SPIE* **2004**, *5516*, 79.

(29) MieCalc − online Mie scattering calculator; www.lightscattering.de/MieCalc/eindex.html.

DOI: 10.1021/acsphotonics.5b00009
ACS Photonics 2015, 2, 622−627

(30) Porres, L.; Holland, A.; Palsson, L.; Monkman, A.; Kemp, C.; Beeby, A. Absolute Measurements Of Photoluminescence Quantum Yields Of Solutions Using An Integrating Sphere. *J. Fluoresc.* **2006**, *16*, 267−273.
(31) Laser manufacturer (Continuum) specification; www.gmp.ch/pdf/Datasheets/Continuum/Panther_EX_OPO.pdf.
(32) Zheludev, N.; Bennett, P.; Loh, H.; Popov, S.; Shatwell, I.; Svirko, Y.; Gusev, V.; Kamalov, V.; Slobodchikov, E. Cubic Optical Nonlinearity Of Free Electrons In Bulk Gold. *Opt. Lett.* **1995**, *20*, 1368.
(33) Hendry, E.; Hale, P.; Moger, J.; Savchenko, A.; Mikhailov, S. Coherent Nonlinear Optical Response Of Graphene. *Phys. Rev. Lett.* **2010**, 105.
(34) Boyd, R. *Nonlinear Opt.*; Academic Press: San Diego, CA, 2003.

DOI: 10.1021/acsphotonics.5b00009
ACS Photonics 2015, 2, 622−627